A COMPARATIVE STUDY OF MISMATCH PROJECTORS IN CONE BEAM CT

Shiyu Xie, Alireza Entezari and Arunava Banerjee

Email: {shiyu.xie, entezari, arunava}@ufl.edu

ABSTRACT

Fast projectors are widely used for reducing the computational costs of modeling X-ray optics in iterative CT reconstruction. This study examines the strengths of state-of-the-art GPU-based projectors in mismatch settings, where forward and back-projection combine the computational advantages of different methods in traditional iterative methods as well as momentum based methods. Specifically, we consider the Siddon, voxel-driven, and distance-driven projectors together with the recently introduced convolutional nonseparable footprint (CNSF) projector under realistic conditions that incorporate effects of the Beer-Lambert law as well as discretization errors. Our experiments suggest that specific mismatched combinations can achieve faster convergence and better image quality than some commonly-used matched projectors. We assess the performance of different projector combinations in terms of both reconstruction runtime and accuracy. These findings provide insights into selecting optimal GPU-based projector pairs, aiming to achieve an ideal balance between speed and quality in CT reconstruction.

***Index Terms*—** GPU-based projectors, CT reconstruction, iterative method, voxel-driven projector, distance-driven projector, Siddon projector, convolutional nonseparable footprint projector

1. INTRODUCTION

Model-Based Iterative Reconstruction (MBIR) algorithms are essential in low-dose and limited-view X-ray imaging applications. While they are known to improve imaging quality from low-dose data, they are, however, computationally expensive [1]. The computational bottleneck in MBIR algorithms lies in modeling the X-ray optics, known as the forward model, that is computed in each step of iteration during forward and back-projection. These computational costs make MBIR prohibitively expensive particularly in cone beam geometry at clinically relevant resolutions.

To reduce the computational costs of modeling X-ray optics, fast projectors introduce various approximations to the forward model and provide speedups at the expense of deviations from realistic models of X-ray optics. These deviations often impact the quality of reconstructed images that can be observed in low-dose applications [2]. Commonly used fast projectors include traditional approaches such as Siddon's, voxel-driven or distance-driven projectors [3], and more recent projectors such as separable footprints [4] and convolutional non-separable footprints [2]. As approximations in each projector is different each approach strikes a different balance between computational cost and the accuracy of modeling X-ray optics in forward and back-projection.

To derive computational advantages, it is possible to combine forward projection of one projector with a back-projection of another projector, known as a mismatch projector [5, 6, 7]. In the mismatched setting, convergence of iterations is not necessarily guaranteed; however, it has been shown that mismatch projectors can be effective in accelerating error reduction during the early stages of iterations. It has also been observed that the requirements for accuracy in backward projection might be less strict than previously thought [7]. However, these observations were made under idealistic conditions using parallel beam geometry, leaving several critical aspects unexplored in realistic settings.

This paper evaluates the performance of mismatched projectors in cone beam geometry under realistic conditions where discretization errors and the nonlinearity of the Beer-Lambert law [1] are known to affect reconstruction quality. We also explore the stability and effectiveness of momentum-based optimization algorithms, together with traditional iterative methods in the context of mismatched projectors - an aspect that lacks theoretical validation but has practical significance for reducting reconstruction time. Our analysis focuses on both computational efficiency and reconstruction accuracy, providing insights into practical trade-offs in clinical CT reconstruction. The analysis aims to identify suitable combinations of forward and backward projectors that can improve reconstruction speed while maintaining image quality that can, in turn, improve usability of MBIR in clinical settings.

2. METHODS

This section introduces the key components of the reconstruction pipeline we study, namely the GPU-based projectors and the iterative algorithms used for CT reconstruction.

This project was supported in part by the NSF grant CCF-2210866.

2.1. Fast Projectors

Siddon Projector The Siddon projector [8] is a ray-tracing algorithm that calculates voxel contributions to the detector by determining ray intersections with the image coordinate system. The algorithm focuses on directly intersected voxels, enhancing efficiency. For each intersected voxel, the method measures the ray's path length, which determines the voxel's impact on the projection value.

While the Siddon projector does not account for detector blur effects, it is efficient and easily implemented on GPUs due to its simplicity. The GPU-based implementation of Siddon's forward projection is particularly efficient and is widely used in applications [9].

Voxel-Driven Projector The voxel-driven projector [10, 11] computes the contribution of each voxel to the detector pixels by iterating through all voxels in the volume. It determines the affected detector pixels for each voxel and calculates the weight of a voxel's contribution based on the intersection length of the ray connecting the voxel center to the source with the detector pixel.

This method employs a geometrical approach to compute the voxel-pixel mapping, using the projection coordinates of the voxel center on the detector plane and interpolation techniques to distribute the voxel's value to the surrounding detector pixels. While the voxel-driven projector does not account for detector blur effects, its back-projection is efficiently implemented on the GPU [9].

Distance-Driven Projector The Distance-Driven (DD) projector [12] for cone beam CT calculates the intersection points between the voxel and the lines connecting the source to the midpoints of the four edges of each detector cell. These intersection points can be approximately viewed as forming a rectangle. This approach also provides an approximate simulation of the detector blur effect, enhancing the accuracy in practical applications. The weight of a voxel's contribution to a detector pixel is determined by the overlap area, calculated using simple geometric operations on the mapped boundaries. Due to its efficiency on GPU [13], this method is used for both forward and backward projections in our study.

Convolutional Non-Separable Footprints The CNSF projector [14, 2] derives the exact line integrals of pixel/voxels in the sinogram domain using an algebraic framework for directional convolution in the continuous domain. The integration over the detector cell is approximated by back-projection of the detector cell on a central slice through the pixel/voxel resulting in a directional convolution in the image space. The line integrals of the directionally-blurred pixel are then computed exactly by piecewise polynomial functions that are efficiently evaluated during forward and back projection.

2.2. Iterative Methods

Given a projector, the forward projection during iterations is denoted by A and back-projection is denoted by A^T. Let x_k denote the image estimate at the k-th iteration, and z_k be an auxiliary sequence when needed.

The Simultaneous Iterative Reconstruction Technique(SIRT) SIRT [15] is widely used for iterative reconstruction that is based on the algebraic reconstruction technique (ART). The iterative update formula is:

$$\begin{aligned} x_{k+1} &= x_k + CA^T R\,(y - Ax_k) \\ C_{jj} &= \frac{1}{\sum_j a_{ij}} \quad R_{ii} = \frac{1}{\sum_i a_{ij}} \end{aligned} \tag{1}$$

where: $R_{ij} = C_{ij} = 0$ for $i \neq j$ and a_{ij} denote the elements of A. These matrices C and R are diagonal matrices that contain the sum of the columns and rows of the projector, respectively.

Fast Gradient Method (FGM) FGM [16] is a first-order optimization algorithm that leverages momentum to accelerate convergence. The iterative update formula is:

$$z_{k+1} = x_k - 2\alpha A^T(Ax_k - b) \tag{2}$$

$$t_{k+1} = \frac{1 + \sqrt{1 + 4t_k^2}}{2} \tag{3}$$

$$x_{k+1} = z_{k+1} + \frac{t_k - 1}{t_{k+1}}(z_{k+1} - z_k) \tag{4}$$

where α is the step size, and t_k is a sequence controlling the momentum.

Optimized Gradient Method (OGM) OGM [17] is a variant of FGM with potentially faster convergence. OGM is identical to FGM except for an additional term in the x_{k+1} update:

$$x_{k+1} = z_{k+1} + \frac{t_k - 1}{t_{k+1}}(z_{k+1} - z_k) + \frac{t_k}{t_{k+1}}(z_{k+1} - x_k) \tag{5}$$

3. EXPERIMENTS

We set up a cone-beam flat detector X-ray CT system and conducted experiments using the 3D Shepp-Logan phantom. To account for discretization errors and the nonlinearity of the Beer-Lambert law, we generated projection data using analytical line integrals. To simulate the effects of unmatched projectors in low-dose scenarios, we utilized data from 120 views. For the cone-beam experiment, we employed a field of view (FOV) of $64\ \mathrm{mm} \times 64\ \mathrm{mm} \times 64\ \mathrm{mm}$, with a resolution of $512 \times 512 \times 512$. The simulation was performed on a flat detector cone-beam CT system with a source-to-detector distance (D_{sd}) of 167.125 mm and a source-to-object distance (D_{so}) of 121.25 mm. To cover this FOV, each view

had an 801×801 detector array with a detector cell size of $0.125\ \text{mm} \times 0.125\ \text{mm}$.

In the following experiment, we evaluate the GPU runtime performance of unmatched projector pairs, the convergence rates of three iterative algorithms, and the visualization of the reconstruction results.

3.1. GPU Performance

Due to the varying implementation efficiencies of different projectors on the GPU, we currently have Siddon (a type of ray-driven) forward projector, voxel-driven backward projector, distance-driven forward and backward projectors, and CNSF forward and backward projectors implementations. We present the GPU runtime of these projectors under the settings mentioned before, as well as the total execution time when there is a mismatch. The experiments were conducted using an NVIDIA GeForce RTX 3090 GPU.

Method	**Runtime (seconds)**
Siddon Forward Projection	3.905
Pixel Driven Back Projection	0.694
Distance Driven Forward Projection	1.365
Distance Driven Back Projection	0.930
CNSF Forward Projection	4.994
CNSF Backward Projection	1.683

Table 1. Average Runtime for Different Forward Projection and Backward Projection Methods

The result shows that Distance Driven performs fastest in forward projection, while Pixel Driven in backward projection.

3.2. Reconstruction Error

We ran three iterative algorithms: SIRT, FGM, and OGM, each for one hundred iterations. We recorded the RMSE between the reconstructed image and the original Shepp-Logan phantom after each iteration. For all methods, we initialized the reconstruction with a zero vector $x_0 = 0$, ensuring identical initial backward error across all algorithms.

To determine step sizes for FGM and OGM, we estimated the Lipschitz constant using the power method. This method iteratively approximates the largest eigenvalue of $A^T A$. For optimal convergence, we set the step size for both FGM and OGM to the inverse of this Lipschitz constant, approximately 8×10^{-6}. These parameter choices were made to ensure convergence for each method.

Based on the RMSE results, we observed the following:

- Among the three algorithms tested, matched CNSF projectors demonstrated the best performance, exhibiting both the fastest convergence rate and achieving minimal backward error.
- In mismatched settings between CNSF and other projectors, the backward error convergence rate was enhanced.

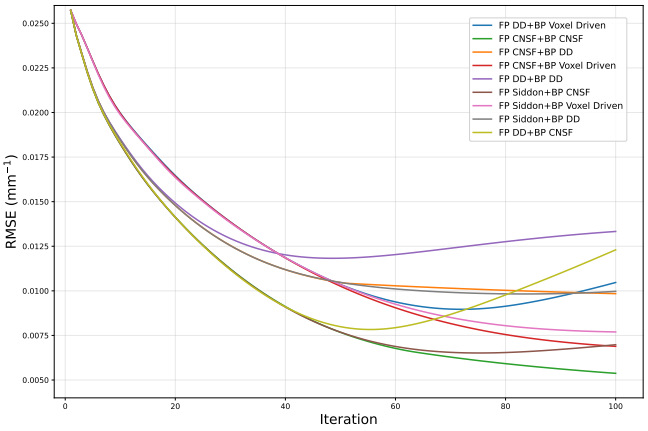

Fig. 1. RMSE of Different Projector Mismatches using Fast Gradient Method (FGM)

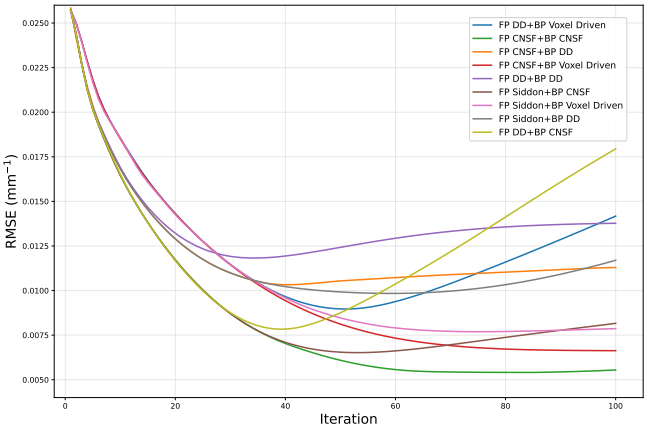

Fig. 2. RMSE of Different Projector Mismatches using Optimized Gradient Method (OGM)

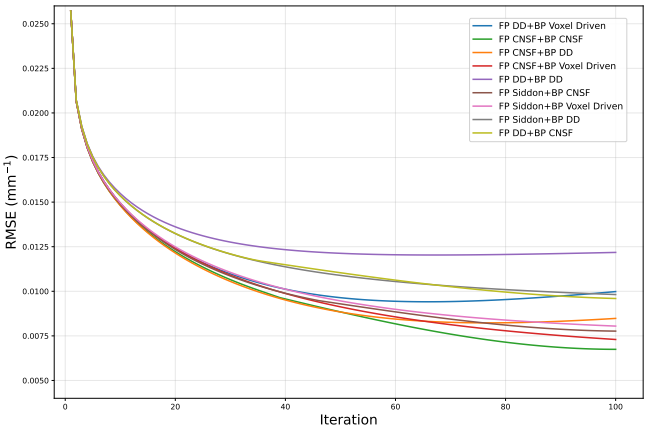

Fig. 3. RMSE of Different Projector Mismatches using Simultaneous Iterative Reconstruction Technique (SIRT)

Notably, across all three algorithms, implementing CNSF as a mismatched forward projector consistently performed better compared to its implementation as a mismatched backward projector.

- Comparative analysis of the three algorithms revealed that OGM initially exhibited the most rapid error descent rate. However, beyond several iterations, it showed an accelerated increase in backward error. In contrast, SIRT displayed robust performance under mismatched projector configurations, maintaining stable backward error descent without experiencing significant error increase.

It is worth mentioning that the experiments described were conducted with views set to 120. However, we also experimented with views ranging from 100 to 180, with intervals of 20, while keeping other parameters constant and employing the power method for selecting the step size. The trends observed in these three iterative methods are similar to those depicted in Figures 1 to 3, suggesting that the experimental results have general applicability.

3.3. Reconstruction Results

Under the settings mentioned, we visualized the reconstruction differences in the X, Y, and Z slices compared to the original Shepp-Logan phantom with the top four projector combinations with the lowest RMSE across all three algorithms.

The results indicate that when CNSF is used as the forward projector, differences in reconstruction quality are very similar; however, when using Siddon as the forward projector with CNSF as the backward projector, significant artifacts occur within the interior of the phantom. In contrast, the combination of Siddon forward projector and voxel-driven backward projector leads to more obvious errors along the phantom boundaries. These observations suggest that the forward projector has a greater impact on the reconstruction quality.

4. CONCLUSIONS

In this paper, we have presented experimental results considering projector mismatches under the Beer-Lambert law, revealing outcomes that differ from conventional expectations.

It was observed that projectors not accounting for detector blur (Siddon/Voxel driven), those approximating detector blur (distance-driven), and those exactly computing detector blur (CNSF) exhibit significant differences when mismatches occur. From the RMSE plots across three iterative algorithms and visualization results, we observed that selecting a forward projector capable of accurately computing detector blur is more crucial in reducing reconstruction errors in mismatch experiments. When computation time is a consideration, matching such forward projectors with more efficient backward projectors (voxel-driven/distance-driven) can balance reconstruction quality and efficiency requirements.

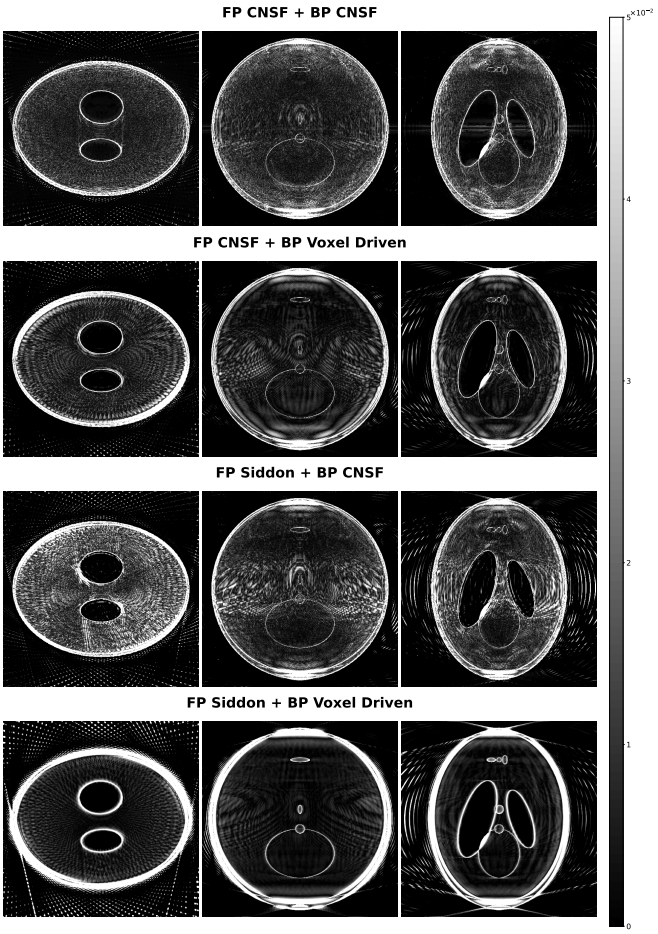

Fig. 4. Visualization of absolute differences between the reconstructed images and the original 3D Shepp-Logan phantom using various combinations of forward/backward projectors after 80 iterations with the OGM algorithm. Each row shows the X, Y, and Z axis slices (from left to right) for different projector combinations. Each row shows the X, Y, and Z axis slices (from left to right) for different projector combinations: CNSF/CNSF, CNSF/Voxel-Driven, Siddon/CNSF, and Siddon/Voxel-Driven (from top to bottom).

Furthermore, we tested these mismatched projectors with three iterative algorithms. The results show that under the OGM algorithm, the presence of momentum enables the fastest RMSE decrease among the three algorithms in the early stages; however, SIRT, by considering the norms of both forward and backward projectors in each iteration, can achieve more stable error reduction in mismatched settings.

Regarding GPU runtime, the time difference between various mismatch methods can exceed twice that of matched pairs. In practical applications, one can balance runtime and accuracy to select the most suitable mismatch combination. This paper provides references for choosing projector pairs, aiding in the effective application of these methods.

5. REFERENCES

[1] Jeffrey A. Fessler, "Statistical image reconstruction methods for transmission tomography," *Handbook of medical imaging*, vol. 2, pp. 1–70, 2000.

[2] Kai Zhang and Alireza Entezari, "Convolutional forward models for X-Ray computed tomography," *SIAM Journal on Imaging Sciences*, vol. 16, no. 4, pp. 1953–1977, 2023.

[3] Yulia Levakhina, *Three-Dimensional Digital Tomosynthesis: Iterative reconstruction, artifact reduction and alternative acquisition geometry*, Springer, 2014.

[4] Yong Long, Jeffrey A Fessler, and James M Balter, "3d forward and back-projection for x-ray ct using separable footprints," *IEEE transactions on medical imaging*, vol. 29, no. 11, pp. 1839–1850, 2010.

[5] Per Christian Hansen, Ken Hayami, and Keiichi Morikuni, "Gmres methods for tomographic reconstruction with an unmatched back projector," *Journal of Computational and Applied Mathematics*, vol. 413, pp. 114352, 2022.

[6] Tommy Elfving and Per Christian Hansen, "Unmatched projector/backprojector pairs: Perturbation and convergence analysis," *SIAM Journal on Scientific Computing*, vol. 40, no. 1, pp. A573–A591, 2018.

[7] Gengsheng L Zeng and Grant T Gullberg, "Unmatched projector/backprojector pairs in an iterative reconstruction algorithm," *IEEE transactions on medical imaging*, vol. 19, no. 5, pp. 548–555, 2000.

[8] Robert L Siddon, "Fast calculation of the exact radiological path for a three-dimensional ct array," *Medical physics*, vol. 12, no. 2, pp. 252–255, 1985.

[9] Ander Biguri, Manjit Dosanjh, Steven Hancock, and Manuchehr Soleimani, "Tigre: a matlab-gpu toolbox for cbct image reconstruction," *Biomedical Physics & Engineering Express*, vol. 2, no. 5, pp. 055010, 2016.

[10] Richard Gordon, Gabor T Herman, and Steven A Johnson, "Image reconstruction from projections," *Scientific American*, vol. 233, no. 4, pp. 56–71, 1975.

[11] TM Peters, "Algorithms for fast back-and re-projection in computed tomography," *IEEE transactions on nuclear science*, vol. 28, no. 4, pp. 3641–3647, 1981.

[12] Bruno De Man and Samit Basu, "Distance-driven projection and backprojection," in *2002 IEEE Nuclear Science Symposium Conference Record*. IEEE, 2002, vol. 3, pp. 1477–1480.

[13] Rui Liu, Lin Fu, Bruno De Man, and Hengyong Yu, "Gpu-based branchless distance-driven projection and backprojection," *IEEE transactions on computational imaging*, vol. 3, no. 4, pp. 617–632, 2017.

[14] Kai Zhang and Alireza Entezari, "A convolutional framework for forward and back-projection in fan-beam geometry," in *2019 IEEE 16th International Symposium on Biomedical Imaging (ISBI 2019)*. IEEE, 2019, pp. 1455–1458.

[15] Jeannot Trampert and Jean-Jacques Leveque, "Simultaneous iterative reconstruction technique: Physical interpretation based on the generalized least squares solution," *Journal of Geophysical Research: Solid Earth*, vol. 95, no. B8, pp. 12553–12559, 1990.

[16] Yurii Nesterov, "A method for unconstrained convex minimization problem with the rate of convergence o (1/k2)," in *Dokl. Akad. Nauk. SSSR*, 1983, vol. 269, p. 543.

[17] Donghwan Kim and Jeffrey A Fessler, "Generalizing the optimized gradient method for smooth convex minimization," *SIAM Journal on Optimization*, vol. 28, no. 2, pp. 1920–1950, 2018.

6. COMPLIANCE WITH ETHICAL STANDARDS

This is a numerical simulation study for which no ethical approval was required.

7. ACKNOWLEDGMENTS

This project was supported in part by the NSF grant CCF-2210866. The authors have no relevant financial or non-financial interests to disclose.